Self-assembly of single PEO-PPO-PEO triblock copolymeric system for Curcumin drug

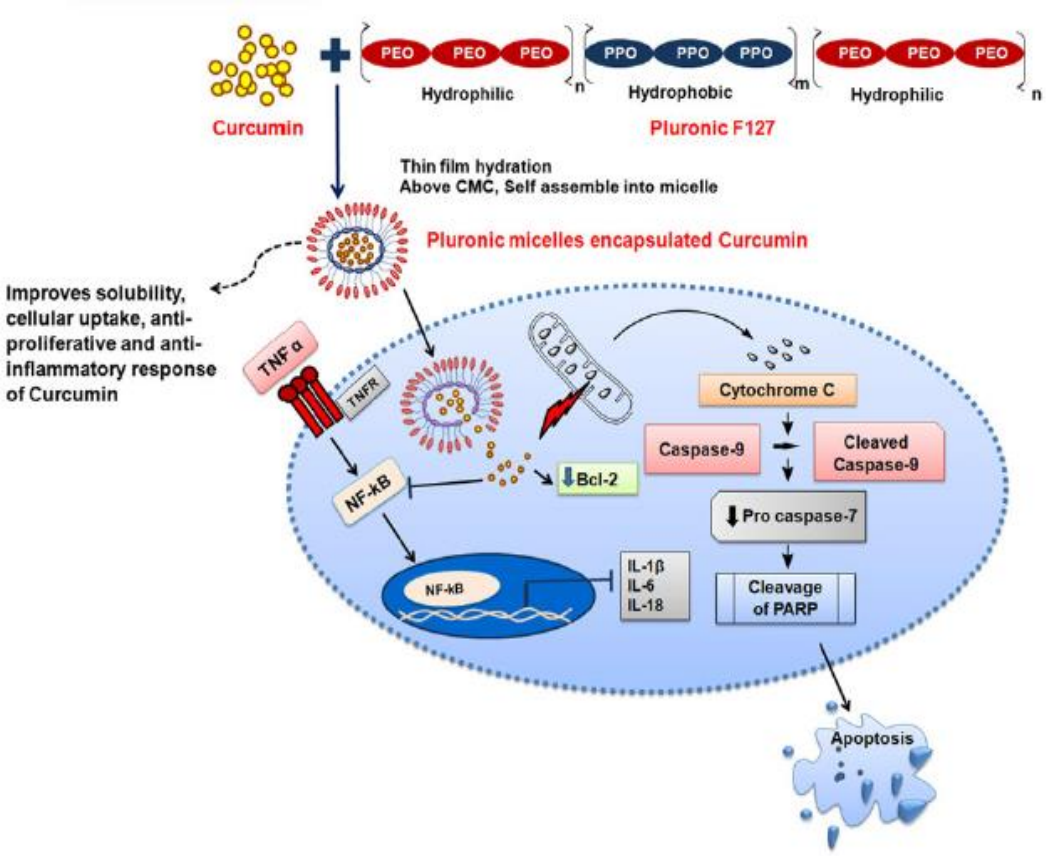

This chapter is a part of paper published in ***Cancer Reports****, e1133, 2018 (Wiley), https://doi.org/10.1002/cnr2.1133*

2.1: Introduction

Cancer always the main causes of death worldwide and is of great concern, not only among the chemists, biologists, and pharmacists but increasingly among the general population. Most commonly surgery, radiation, and chemotherapy are the treatments of cancer. Normally for chemotherapy, various agents such as cisplatin, mitoxantrone, estramustine, doxorubicin, etoposide, vinblastine, paclitaxel, vinorelbine, or a combination of these drugs have been widely used in treatment [1-3]. However, these agents show unexpected toxicity to normal organs and the patients suffer from other side effects. Furthermore, most of the chemotherapeutic agents may not kill all cancer cells and their repeated administration develops drug resistance or androgen refractory stage in the body which is difficult to cure [4]. Therefore, it is a need to develop formulations with no or minimal side effects on normal organs. In this context, a variety of natural compounds have been investigated in the treatment of cancer.

The Indian solid gold, Curcumin is a hydrophobic polyphenol derived from turmeric: the rhizome of the herb *Curcuma longa*. Chemically, it is a bis-α, β-unsaturated β-diketone (commonly called diferuloylmethane) that exhibits keto-enol tautomerism, having a predominant keto form in acidic and neutral solutions and a stable enol form in alkaline media. The chemical structure of curcumin is shown in Scheme.2.1. It has been receiving considerable attention because of its putative cancer prevention and anticancer activities which are mediated through influencing multiple signaling pathways [5,6].

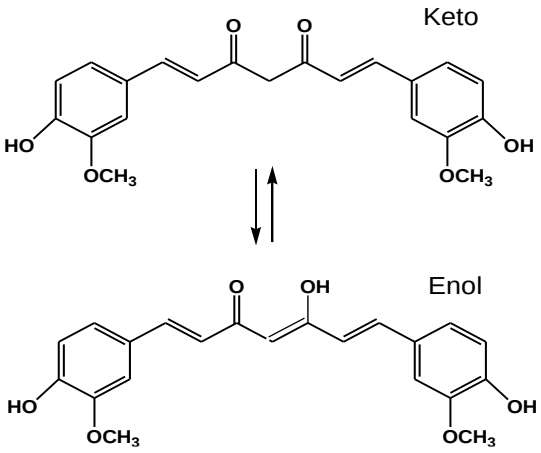

Scheme.2.1: Molecular structure of curcumin drug.

Recently Gillies et al [7] have described the physicochemical properties of curcumin, including its chemical structure, stability, and degradation products as a function of pH and temperature. They also explain the proposed mechanisms by the way the curcumin drugs exhibits anticancer activity. It has been reported that curcumin shows a wide range of pharmacological applications such as anti-inflammation, anti-human immunodeficiency virus, antimicrobial, antioxidant, antiparasitic, antimutagenic with low or no intrinsic toxicity [8-12].

In spite of this wide spectrum of pharmacological properties, the clinical applications of curcumin have been limited due to low solubility in aqueous media (11 ng/mL in aqueous buffer pH 5.0) and rapid degradation at physiological pH [13,14]. Also, the absorption of curcumin in gastrointestinal(GI) tract is very low, for example, the absolute oral bioavailability in a rat is only about 1% [9]. Although the solubility of hydrophobic curcumin can be improved by alkalization of the aqueous solution, the compound will be rapidly degraded at this medium [15,16]. Curcumin is also photochemically unstable. Therefore, the formulation which can solubilize and stabilize curcumin prior to administration is essential to provide sufficient photoactivity during treatment. Various formulations of curcumin have been developed, such as β-cyclodextrin inclusion complex [13], PLGA nanoparticles [17], nanosuspension [18], nanospheres [19], polymeric nanoparticles [20]. A recent study showed that encapsulation of hydrophobic drugs into polymeric micelles is one of the most attractive alternatives for better formulations [21]. Amphiphilic block copolymers form core-shell nanosized aggregates/micelles which can solubilize poorly water-soluble drugs and improve their bioavailability and protect from inactivation in biological media [22].

The class of ABA triblock copolymers commercially available as Pluronic® (the non-proprietary name "Poloxamers") offers a pool of more than 50 amphiphilic [23], water-soluble and polymorphic materials [A=hydrophilic poly(ethylene oxide) (PEO) block and B=hydrophobic poly(propylene oxide) (PPO) block]. Structural studies show that Pluronic block copolymer can self-assemble into spherical micelle comprising a hydrophobic inner core of PPO and hydrophilic PEO as outer corona shell [24]. Such Pluronic micelles (typically smaller than 50 nm) possess a core-shell structure in aqueous media and poorly water-soluble drugs can be incorporated into the PPO hydrophobic core and protected from

interaction with cells and proteins through a surrounded shell of PEO [22,24]. These Pluronic micelles have been largely utilized to deliver many known hydrophobic drugs with improved bioavailability and efficacy [22,25-28]. Pluronic block copolymers can also improve oral absorption of drugs, further indicating that they are a promising nanocarrier for drug delivery applications [28].

The encapsulation of curcumin drug using self-assembly of Pluronic polymers (Pluronic F127 and Pluronic F68) have successfully reported by Sahoo et al [29]. The encapsulation of curcumin molecules into Pluronic micelles was dependent on drug-to-polymer ratio and hydrophobicity of Pluronic itself. Tonnesen et al [15,30] have also studied on the solubility and hydrolytic as well as photochemical stability of curcumin drug in the presence of various Pluronics. The solubility of curcumin has increased 100–1000 times, and the hydrolytic stability of curcumin improved 50–400 times by addition of Pluronics. Mohanty et al [31] have also successively prepared curcumin loaded nanoparticles composed of glycerol monooleate and Pluronic F127. The entrapment efficiency was around 90% and the size of the nanoparticles almost 192 nm with a high negative zeta potential (-32 mV) that ensured long term stability and prevent aggregation of the particles. When dispersed in a buffer, these nanoparticles enhanced the stability of curcumin by protecting it against hydrolysis. Not only that the mixture of Pluronic block copolymers (Pluronic P123 and Pluronic F68) have been also studied by Zhao et al [32] to optimize the formulation of curcumin drug. The average size of the mixed micelles was 68 nm, and the encapsulation efficiency and loading capacity for curcumin were 87% and 7%, respectively. It has shown that 50% of the loaded curcumin released from the mixed micelles in 72 h demonstrating that this formulation had sustained-release properties. Samanta et al [33] conducted a molecular dynamic study of curcumin with Pluronic block copolymers, specifically Pluronic P85, and observed that the hydrophobic PPO chains wrap around the curcumin molecule leaving the hydrophilic PEO chains exposed and thus resulting in better solvation of curcumin drug in water. Although there were few reports on the effect of Pluronic on the in vitro cytotoxicity of curcumin [29], best of our knowledge no one investigated the structural insights of curcumin incorporated Pluronic micelles.

The purpose of this work was to elucidate Pluronic F127, the most efficient copolymer in the category, for improved bioavailability of curcumin. The curcumin-

incorporated Pluronic F127 micelles (PMsCur) has been developed using a thin film hydration method without any additional cryoprotectants. The physicochemical behavior, particle size, drug loading and interaction of PMsCur have successfully investigated through advanced techniques like small- angle neutron scattering (SANS), dynamic light scattering (DLS), powdered X-ray diffraction(XRD), Fourier infrared spectroscopy (FTIR), differential scanning calorimetry (DSC) and UV-Visible spectroscopy (UV-VIS). In vitro release and stability of PMsCur was also investigated for the better understanding of the formulations.

2.2: Experimental Section

2.2.1: Materials

PEO-PPO-PEO triblock copolymer (Pluronic F127) was purchased from Sigma-Aldrich (St.Luice, MO, USA) and used as received. The molecular characteristics of the Pluronic F127 are listed in Table.2.1.

Table .2.1: Molecular characteristics of Pluronic F127

MW, $g.mol^{-1}$	%EO	n EO	n PO	HLB	CP,°C @ 1 wt%	CMC, wt%
12600	70	100	65	22	>100°	0.06[#]

[#] reported from ref.34

Curcumin from *Curcuma longa* (Turmeric) was the product of Sigma-Aldrich. The specification of the curcumin drug is presented in Table.2.2.

Table.2.2: Specification of curcumin drug

Appearance	Code Name	MW, $g.\ mol^{-1}$	*pka* value	Partition coefficient (*P*)
	Cur	368.38	7.8	2.85

2.2.2: Determination of critical micelle concentration (cmc)

The cmc determination of the Pluronic F127 carried out using pyrene as a probe by the UV–Visible spectroscopy technique at room temperature (30°C) [35]. Here, the required amount of pyrene was dissolved in methanol and added to the Pluronic F127 solutions in the ratio of 1:100 (50 µL: 5 mL). Thus, solutions of Pluronic F127 ranging from 0.0001 to 10 wt% concentrations and a fixed amount of 1×10^{-4}M of pyrene were obtained. The absorbance measurements of the prepared samples were taken after around 24 h with proper filtration using Shimadzu (UV-2450) UV–visible double beam spectrophotometer with matched pair of Stoppard fused silica cells of 1 cm optical path length. Fig.2.1 shows the simple absorbance spectra of pyrene in water. Due to multiple rings, the five-strong peaks at 239, 260, 272, 319 and 334 nm, of pyrene are clearly visible in the spectrum. The absorbances of the pyrene peaks increase by increasing the Pluronic F127 concentrations.

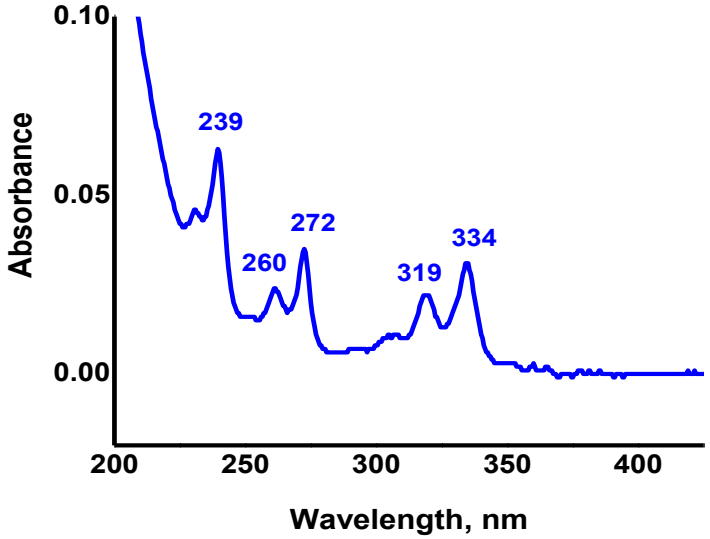

Fig.2.1: Absorbance spectra of pyrene

So, the cmc obtained from the combined spectra by monitoring the absorbance values at different peaks of pyrene for different concentrations of Pluronic F127. The concentration of the Pluronic F127 varied both from below to above the cmc and curves of intensity ratio versus concentration of Pluronic F127 (wt%) used for the determination of the cmc. The inflection point of the intensity ratio versus concentration of the Pluronic F127 plot taken as the cmc of the Pluronic F127.

2.2.3: Phase-solubility experiments

2.2.3.1: Calibration of curcumin drug

The analysis was performed by first scanning the curcumin (1 µg/mL) solution in the ultraviolet range between 200 to 800 nm and determining its λmax. Suitable aliquots of the stock solution of curcumin pipetted out into 10 mL volumetric flasks and the volume was made up to 10 mL with ethanol to give final concentration ranging from 1 to 5×10^{-4} mg/mL. The solutions mixed using vortex mixer and its absorbances measured at λmax 425 nm using ethanol as a reference on UV-visible Spectrophotometer (Shimadzu, Japan, UV-2450) and the calibration curve was plotted (shown in Fig.2.2). The above procedure was repeated three

times. Parameters indicating linearity for the used UV spectrometric method of analysis for curcumin drug are shown in Table.2.3.

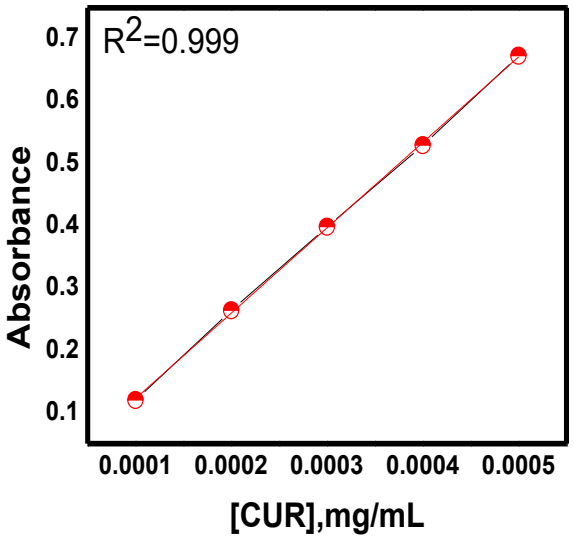

Fig.2.2: Calibration curve of curcumin in ethanol as solvent.

Table .2.3: Parameters for UV-VIS spectroscopy analysis for curcumin drug in ethanol.

Parameter	Result
λ_{max}	425 nm
Linearity range	1-5×10^{-4} mg/mL
Regression equation	y=a+b*c
Correlation coefficient(R^2)	0.9996

2.2.3.2: The solubility of curcumin drug in Pluronic F127 micelles

Phase solubility experiments were carried out by UV-VIS spectroscopy method on UV–visible double beam spectrophotometer(Shimadzu, Japan, UV-2450). Saturated curcumin-loaded Pluronic F127 solutions were prepared in glass vessels by mixing the excess powdered drug into Pluronic F127 solution and stirring with 200 rpm at constant temperature (37°C) for 2 days. The solutions were filtered (Millipore, 0.45µm) to remove the unsolubilized drug. The amount of drug solubilized was determined by measuring absorbance at λ=425 nm. In solubilization experiments, the filtered solution was diluted 60–120 times with ethanol, the amount of water after dilution very much low to allow direct use of the calibration plot. Each solubility value was determined in triplicate and the results are

reported as the mean of the three. This experiment further took into consideration of the Pluronic F127 concentration in the synthesis of curcumin-incorporated Pluronic F127 micelles (PMsCur).

2.2.4: Synthesis of curcumin-incorporated Pluronic F127 micelles (PMsCur)

Curcumin-incorporated Pluronic F127 micelles (PMsCur) were synthesized through the Thin-film hydration method [29] as shown in the flowchart (Scheme.2.2). Briefly, the required amount of Pluronic F127 (fixed 5 wt%) and curcumin drug (0.1 wt%) in a 20 mL of methanol was taken to separate round-bottom flask. The solution was stirred for an hour and poured into the glass plate. The methanol completely evaporated to obtain curcumin-containing solid polymer film. The residual methanol was removed by keeping the plate in a vacuum oven at room temperature for overnight. After that, the solid film was rehydrated with deionized water (pre-warmed at 37°C, pH 7.0) by extensive vortexing and sonicated for 20 minutes to prepare curcumin-incorporated Pluronic micelles. Non-incorporated curcumin was separated by centrifugation (5000 rpm,10 min) and filtration (syringe filter, 0.2µM). Lyophilized PMsCur was obtained by freeze-drying (N_2atm., 0.035 m bar pressure, -55°C temperature). The complete process was performed in dark. The final product, PMsCur was kept in a brown bottle with proper capping.

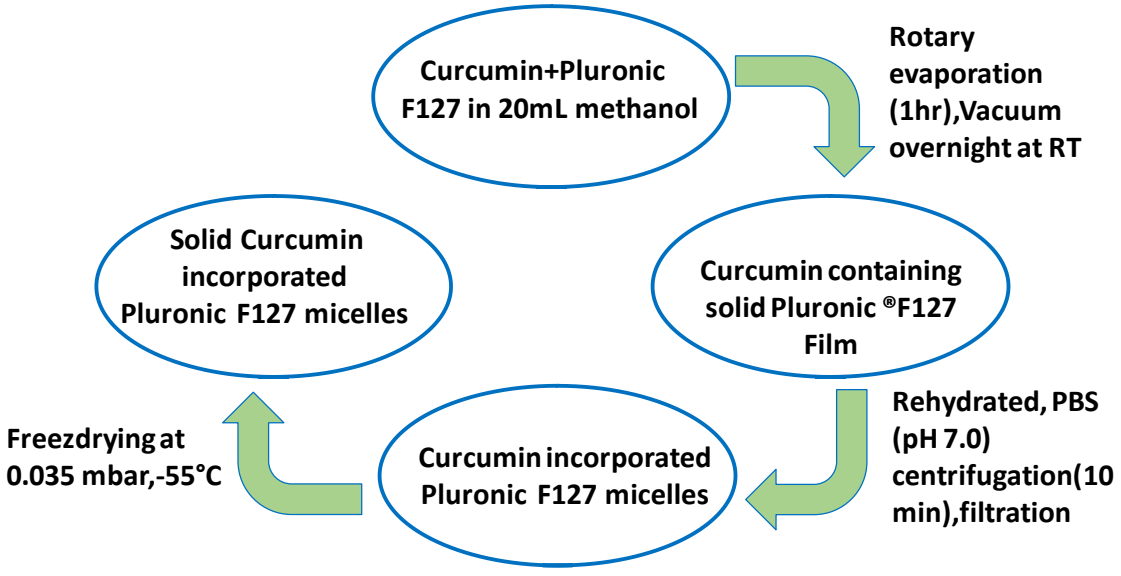

Scheme.2.2: Flow chart of synthesis

2.2.5: Incorporation efficiency(IE) and drug loading(DL) of curcumin in PMsCur

The percentage of curcumin incorporated in the synthesized curcumin-incorporated Pluronic F127 micelles (PMsCur) was determined as follows; 1 mL of aqueous PMsCur solution was centrifuged at 30 min, and the amount of curcumin in the supernatant was measured spectrophotometrically at λ=425 nm. The drug loading and incorporation efficiency were calculated using the following formulas;

$$\text{Incorporation efficiency (\%)} = \frac{W_{loaded}}{W_{added}} \times 100$$

$$\text{Drug Loading (\%)} = \frac{W_{loaded}}{W_{total}} \times 100$$

where W_{loaded} is the curcumin amount entrapped into Pluronic micelles, W_{added} is the initially added curcumin, and W_{total} represents the amount of both curcumin drug and Pluronic F127 in the PMsCur.

2.2.6: Characterization of PMsCur

2.2.6.1: Dynamic light scattering (DLS)

The average particle size (hydrodynamic diameter, Dh) and size distribution of 1 wt% aqueous solutions of PMsCur determined by DLS (Horiba-Zetasizer, SZ-100) with a scattering angle of -173° at 37° C. The freshly prepared sample was placed into a glass cuvette without additional treatment. The size measurement was carried out in triplicate.

2.2.6.2: Small-angle neutron scattering analysis (SANS)

The morphology and other structural detail of Pluronic F127 and PMsCur were determined through small-angle neutron scattering measurements. SANS experiments were performed at the SANS diffractometer at Guide Tube Laboratory, Dhruva Reactor, Bhabha Atomic Research Centre, Mumbai, India [36]. In SANS, one measures the coherent differential scattering cross-section ($d\Sigma/d\Omega$) per unit volume as a function of wave vector transfer Q ($= 4\pi \sin(\theta/2)/\lambda$, where λ is the wavelength of the incident neutrons and θ is the scattering angle). It provides information about the shape and size of the scattering particles in the length scale of 10-1000 Å. The mean wavelength of the monochromatized beam

coming out from the neutron velocity selector was 5.26 Å with a spread of $\Delta\lambda/\lambda$ ~ 15%. The angular distribution of neutrons scattered by the sample is recorded using a 1 m long one-dimensional He3 position sensitive detector. The instrument covers a *Q*-range of 0.017–0.35 Å-1. The temperature of all the samples during the measurements was kept fixed at 37ºC.

The differential scattering cross section per unit volume ($d\Sigma/d\Omega$) as measured for a system of monodisperse particles in a medium can be expressed as[37,38]

$$\left(\frac{d\Sigma}{d\Omega}\right)(Q) = nP(Q)S(Q) + B \ , \ldots\ldots\ldots\ldots\ldots(1)$$

where *n* denotes the number density of particles. *P*(*Q*) is the intraparticle structure factor and *S*(*Q*) is the interparticle structure factor. *B* is a constant term representing the incoherent background, which is mainly due to the hydrogen present in the sample. Intraparticle structure factor *P*(*Q*) is decided by the shape and size of the particle and is the square of single-particle form factor *F*(*Q*).

For a spherical particle of radius *R*, *P*(*Q*) is given by

$$P_p(Q) = 9\left[V\left(\rho_p - \rho_s\right)\frac{\sin(QR) - QR\cos(QR)}{(QR)^3}\right]^2 \ldots\ldots\ldots\ldots(2)$$

$\rho_p$andρ_s are, respectively, the scattering length densities of particle and solvent and *V*is the volume of the particle.

In our measuring systems, the block copolymer micelles have been modeled as core-shell particles with different scattering length densities for core and shell. The structure of these micelles is described using a model consisting of non-interacting Gaussian PEO chains attached to the surface of the PPO core. The form factor of the micelles comprises four terms: the self-correlation of the core, the self-correlation of the chains, the cross term between core and chains, and the cross term between different chains. It is given by[39]

$$P_m(Q) = N_s^2 P_s(Q) + 2N_s P_c(Q) + 2N_s(2N_s - 1)P_{cc}(Q) + 4N_s^2 P_{sc}(Q) \ldots\ldots\ldots\ldots\ldots(3)$$

where *Ns* is the aggregation number of the micelles. The subscript *s* (= core) and *c* (= chain) are used here.

At higher polymer concentrations, an interaction between micelles takes place and a peak arising from the structure factor, *S*(*Q*, *Rhs*, ϕ) where *Rhs* is hard sphere radius and ϕ is volume fraction of micelles, appears in the scattering intensity. *S*(*Q*) describes the interaction

between the particles present in the system and depends on the spatial distribution of micelles, is given by

$$S(Q) = 1 + 4\pi n \int (g(r) - 1) \frac{\sin(Qr)}{Qr} r^2 dr \quad , \ldots\ldots\ldots\ldots\ldots(4)$$

where $g(r)$ is the radial distribution function describing the arrangement of the micelles. In the case of non-ionic micelles, the interparticle interaction (direct correlation between two scattering objects) is obtained using Ornstein–Zernike equation with the Percus-Yevick approximation and employing hard sphere potential between micelles[40], and the analytical form of the structure factor is given as

$$S(Q) = \frac{1}{1 + 24\phi \ (G(x)/x)} \quad , \ldots\ldots\ldots\ldots\ldots(5)$$

where *Rhs* is the hard sphere micellar radius consisting of both the core and the shell which gives the physical size of the micelle, ϕ is the hard sphere volume fraction of the micelles in the solution, and G is a function of $x = 2QRhs$ and ϕ.

In this equation, $G(x)$ is further defined as follows:

$$G(x) = \frac{\alpha(\phi)}{x^2}(\sin x - x\cos x) + \frac{\beta(\phi)}{x^3}[2x\sin x + (2 - x^2)\cos x - 2] + \frac{\gamma(\phi)}{x^5}[-x^4\cos x + 4\{(3x^2 - 6)\cos x + (x^3 - 6x)\sin x + 6)\}] \quad \ldots\ldots\ldots\ldots(6)$$

where

$$\alpha(\phi) = (1 + 2\phi)^2 / (1 - \phi)^4$$

$$\beta(\phi) = -6\phi(1 + \frac{\phi}{2})^2 / (1 - \phi)^2 \quad \ldots\ldots\ldots\ldots\ldots(7)$$

$$\gamma(\phi) = \frac{\phi\alpha}{2}$$

In fitting the experimental scattering data, three unknown parameters, *Rc*, *Rhs* and ϕ have been considered as fitting parameters in the analysis. The aggregation number of micelles, N_{agg} can be calculated using the following expression, $N_{agg} = Vm/Vh$ where Vm (= 4/3 πRc3) is the micellar volume and Vh is the volume of the hydrophobic part of the surfactant monomer.

The polydispersity in size distribution of particle is incorporated using the following integration[41]

$$\frac{d\Sigma}{d\Omega}(Q) = \int \frac{d\Sigma}{d\Omega}(Q,R) f(R) dR + B \text{ , } \ldots\ldots\ldots\ldots\ldots(8)$$

where $f(R)$ is the particle size distribution and usually accounted by a log-normal distribution as given by

$$f(R) = \frac{1}{\sqrt{2\pi}R\sigma} \exp\left[-\frac{1}{2\sigma^2} \left(\ln \frac{R}{R_{med}} \right)^2 \right] , \quad \ldots\ldots\ldots\ldots\ldots(9)$$

where $Rmed$ is the median value and $\sigma$is the standard deviation (polydispersity) of the distribution. The mean radius (Rm) is given by $Rm = R_{med}\exp(\sigma 2/2)$.

The data have been analyzed by comparing the scattering from different models to the experimental data. Throughout the data analysis, corrections were made for instrumental smearing, where the calculated scattering profiles smeared by the appropriate resolution function to compare with the measured data [42]. The fitted parameters in the analysis were optimized using a nonlinear least-square fitting program to the model scattering [43].

2.2.6.3: UV-Visible spectroscopy (UV-VIS)

The UV-visible spectra of free curcumin, Pluronic F127, and PMsCur in water were observed using UV–visible double beam spectrophotometer (UV-2450, Shimadzu, Japan) with matched pair of stoppered fused silica cells of 1 cm optical path length.

2.2.6.4: Fourier transform infrared spectroscopy (FTIR)

FTIR spectra of plain curcumin, Pluronic F127, and lyophilized PMsCur were collected in order to analyze the chemical structure of these compounds and possible changes therein after curcumin loading. Samples were analyzed by spectrophotometer (FTIR-8400S, Shimadzu Co., Kyoto, Japan) using potassium bromide (KBr) pellet method. The spectra were obtained in the frequency range of 4000-400 $cm^{-1}$with a resolution of 4 cm^{-1}**.**

2.2.6.5: Powder X-ray diffraction spectroscopy (PXRD)

Powder X-Ray diffraction (PXRD) patterns were recorded for native curcumin, Pluronic F127 and PMsCur with X-Ray diffractometer (Philips X' Pert MPD, USA) with a scan of 0.50/s in the 2θ range of 2 – 500.

2.2.6.6: Differential scanning calorimetry(DSC)

DSC measurements for the pure curcumin drug, Pluronic F127 and PMsCur were conducted on a Mettler-Toledo, 851e within 30 – 900°C at 10°C/min in a continuous nitrogen flow.

2.2.7: In vitro release study of curcumin from PMsCur

In vitro release study of curcumin from PMsCur was carried out by dialysis bag method. A known concentration (1.0 mg/mL) of curcumin and PMsCur was placed in an activated dialysis bag (MWCO, 10 kDa). The dialysis bag was suspended in the DMEM culture medium. The entire system was kept at 37 ± 0.5°C with constant stirring of 200 ± 2 rpm. At the respective time point, one mL of medium was withdrawn and replaced with fresh medium. The absorbance of curcumin was recorded at 430 nm in a Multimode microplate reader (Molecular Devices, USA) and release of curcumin was quantified using the standard curve of curcumin.

2.2.8: Stability studies of PMsCur

To evaluate the physical stability of PMsCur, a sample was stored at room temperature in the closed chamber and curcumin retention was monitored over the three months after the preparation of PMsCur and quantified using UV-Visible spectroscopy.

2.3: Results and discussion

Amphiphilic molecules tend to associate into micellar systems as a spontaneous process in aqueous solution. The micelles of PEO-PPO-PEO triblock copolymers consist of a desolvated PPO core and a solvated PEO corona. Pluronic F127 is currently approved for pharma applications by the FDA [27]. Owing to high molecular weight with 70% of polyethylene oxide (PEO) units, Pluronic F127 forms micelles at quite high concentration [44,45]. Pluronic F127 has been chosen for this study because of its characteristic micellar behavior. A systematic study of the cmc, cmt, micellization thermodynamics and lyotropic liquid crystalline structure for F127 can be found in the literature [46-50].

2.3.1: CMC of Pluronic F127

The CMC of Pluronic F127 in water was determined using UV-Visible spectroscopy using pyrene as a probe at room temperature. Pyrene is hydrophobic with poor solubility in water but found increased solubility in the micellar environment. When the concentration of polymer is less than cmc, the absorbance changes slightly, and it differs dramatically when it reaches the cmc. The phenomenon is related to the fact that pyrene can move into the inside of the micelles from the aqueous phase once the micelle forms, which results in an alteration in the polarity around [35]. Fig.2.3 shows the plot of intensity ratio (I_1/I_3) versus logarithmic concentration of the Pluronic F127. The CMC value of Pluronic F127 is 0.0698 wt% which is in accordance with the reported one [34].

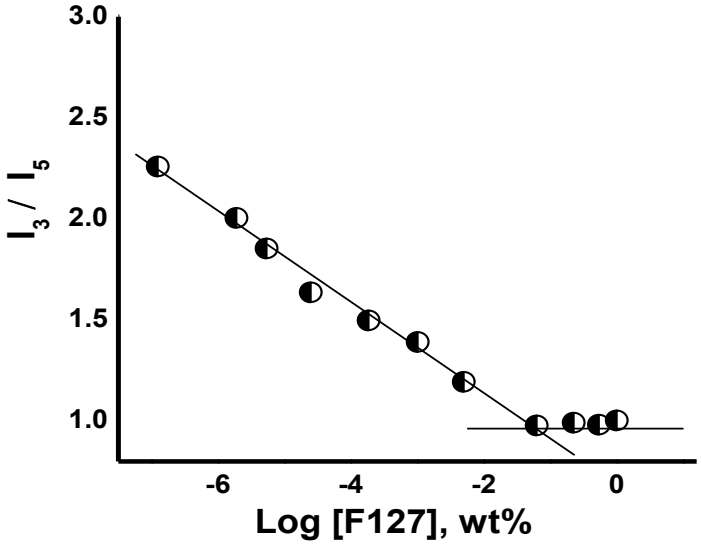

Fig.2.3: Plot of I_3/I_5 versus the log of Pluronic F127 concentration in water at 30°C.

At low concentrations, F127 exists in solution as individual coils (unimers) and thermodynamically stable micelles are formed with increasing F127 concentration. The cmc is very important if one considers using micelles or micellar solution as a drug carrier and/or vehicle. Very low cmc of Pluronic F127 makes these micelles relatively insensitive to dilution and has a longer circulation time compared to conventional surfactant micelles in vivo. Researchers have been studied and found Pluronic F127 is the good candidate for the delivery of the curcumin drug [29,30].

2.3.2: Phase solubility of curcumin in Pluronic F127 solutions

The phase solubility of curcumin in aqueous solutions of Pluronic F127 was monitored using UV-Visible spectroscopy. The plot of drug curcumin solubilized in micellar solutions of Pluronic F127 at body temperature (37°C) is presented in Fig.2.4. The solubilization of drug has significantly increased as the concentration of Pluronic F127 increased. Due to the more number of micelles formed as the increased in F127 concentration, the high drug solubility was observed [30]. The abrupt raising in solubility of curcumin drug from 1.0 wt% to 4.92 wt% and thereafter steady increases at high concentrations(>5,wt%) was clearly observed in the phase solubility curve. Results concluded that one can optimize the concentration of Pluronic F127 nearby 5 wt% for better its applications in the development of curcumin formulations.

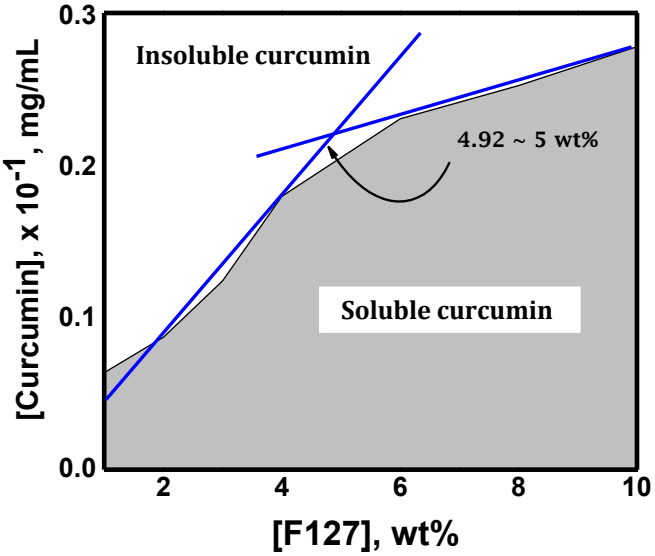

Fig.2.4: Solubility of curcumin in Pluronic F127 solutions at 37°C.

2.3.3: Curcumin-incorporated Pluronic F127 micelles (PMsCur)

The curcumin-incorporated Pluronic F127 micelles (PMsCur) was synthesized by the thin film hydration method, which shows improved aqueous solubility of curcumin drug as compared with the same amount of solid curcumin suspension in water [shown insoluble slurry in Fig.2.5(a)]. When lyophilized PMsCur powder is dissolved in water gave clear yellow colored solution very quickly and easily(Fig.2.5(b)).

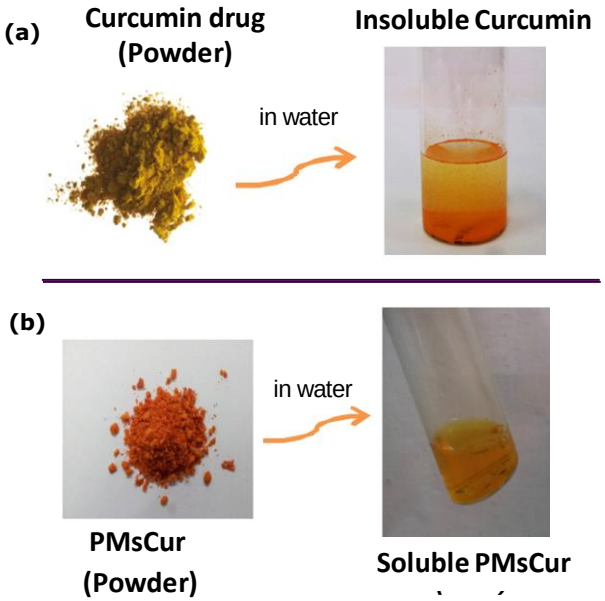

Fig.2.5: (a) Insoluble slurry of curcumin when added in water (b) Synthesized PMsCur dispersed (soluble curcumin) in water.

The properties of PMsCur after curcumin nanoformulation have been reported in Table.2.4. The incorporation efficiency and drug loading of curcumin within the Pluronic F127 micelles were 48.039% and 41.511% based on calculations described in the methods. The aqueous solubility of curcumin in PMsCur is 0.02117 mg/mL, which are quite higher than its aqueous solubility. These results are very effective and the hydrophobic $–CH_3–$ group in the PPO chain of Pluronic F127 provides the main interaction site between the hydrophobic drug and the micelle core of the micelles.

Table.2.4 : Curcumin incorporation in PMsCur.

PMsCur	Curcumin drug is taken	Pluronic F127 (*Wt. fixed 5wt% conc.*)	IE%	DL%	Solubility, mg/mL
	10 mg	50 mg	48.039	41.511	0.02117

2.3.4: Characterization of PMsCur

In a drug delivery system, particle size greatly influences the pharmacokinetics, including the time of circulation, absorption, and distribution [48]. We performed all the study at 37°C, which is well above the cmt (19.5°C) for 5 wt% Pluronic F127 [49]. We have carried out the DLS study of the aqueous solutions of Pluronic F127 and PMsCur. Fig.2.6 shows the intensity versus size in the form of hydrodynamic diameter(Dh) for 5 wt% Pluronic F127 and 1 wt% PMsCur in water at 37°C. The average hydrodynamic diameter of Pluronic F127 alone and PMsCur were 22.3 and 26.0 nm, respectively. The average diameter distribution and PDI result demonstrated a narrow size distribution of PMsCur. These results indicate that the nano size of PMsCur is consistent with low PDI.

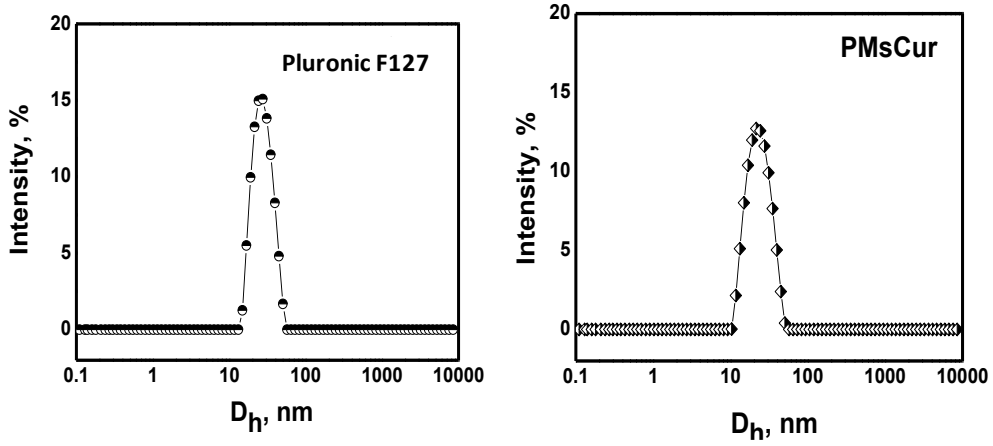

Fig.2.6: Intensity versus hydrodynamic size of 1.0wt% aqueous solution of Pluronic F127 and PMsCur in water at 37°C.

SANS experiments were widely used in the past to study the associative interactions between Pluronic block copolymers and drugs. To further characterize the dispersion quality

of the PMsCur in D_2O, SANS measurements were performed at 37°C (Fig.2.7). For comparison, Pluronic F127 in D_2O at the 5 wt% concentration was also measured. SANS data on Pluronic F127 micelles is well studied [52] but for curcumin incorporated Pluronic F127 micelles are scarce or reported here may first-time in this work. The SANS intensity profile of 5 wt% Pluronic F127 show signatures of both form factor, as well as structural factor, governed scattering. Pluronic F127 micelles are found to be polydispersed micelles with spherical core and Gaussian chains attached to it, interacting with hard sphere potential [53]. The analysis of the data (Table.2.5) reveals an increase in the micellar core radius of Pluronic F127 with curcumin from 55.1 Å to 58.2 Å. The hard sphere radius is 101.1 Å is much larger compared to the core radius is 55.1Å because the interaction radius also involves shell of PEO blocks. The micellar volume fraction, on the other hand, decreases in case of PMsCur. This can be explained based on the fact that micellar solubilization of drug is accompanied by simultaneous micellar dehydration.

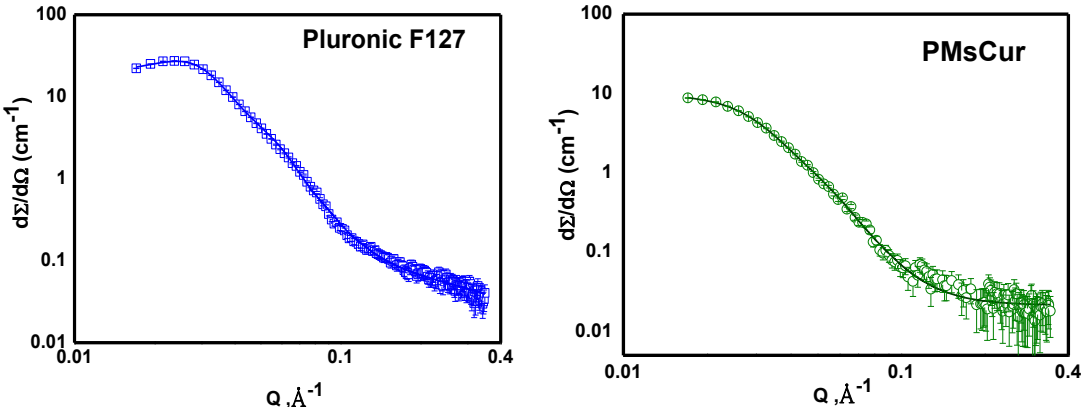

Fig.2.7: SANS intensities of Pluronic F127 and PMsCur in D_2O at 37°C. (The concentration of F127 in both samples was kept 5.0 wt%)

The observed increase in micellar core upon solubilization of curcumin was found due to entrapment of drug in the PPO core and a simultaneous increase in micellar aggregation. The morphology of PMsCur recorded from SANS was spherical and the particle size was also similar to the data observed by DLS.

Table.2.5: Fitted parameters obtained from the analysis of the SANS analysis of Pluronic F127 and PMsCur in D_2O at 37°C.

System	Core radius, *Rc*(Å)	PDI	Radius of gyration Rg, (Å)	Hard sphere radius *Rhs*, (Å)	Volume fraction *Φ*	Aggregation number, N_{agg}
5 wt% F127	55.1	0.36	21.6	101.1	0.17	112
PMsCur	58.2	0.35	21.6	102.9	0.03	130

The incorporation of curcumin drug into Pluronic F127 micelles in PMsCur also confirmed with UV-Visible spectroscopy. The spectrum of an aqueous solution of curcumin was broad and almost lacking any clear maxima. The Pluronic F127 itself was also flat in the spectrum. However, the absorption spectra of PMsCur showed a well-defined maxima at the wavelength of 425 more increase in intensity than a pure drug in water (Fig.2.8). The hydrophobic PPO core of the copolymer F127 effectively encapsulated the curcumin molecules and makes it dispersible in the aqueous media [29].

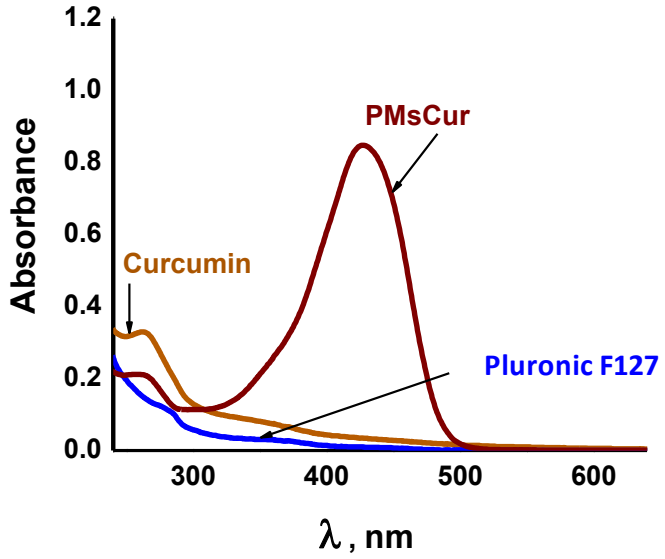

Fig.2.8: Absorbance spectra of curcumin, Pluronic F127 and PMsCur in water (diluted) at 37°C.

In solid state characterization the PMsCur, the spectra of FTIR for curcumin alone, Pluronic F127 and PMsCur are depicted in Fig.2.9. The spectrum of Pluronic F127 showed two major peaks at 1110 cm-1 of C-O-C stretching and 2882 cm^{-1} of –C-H stretching of aliphatic chain. The obvious peaks of –C=C- double bonds stretching of an aromatic moiety

at 1511 cm^{-1} was shown in the IR spectrum of pure curcumin drug. All the peaks of Pluronic F127 were found in the spectrum of PMsCur. The signature peaks at 1585 cm-1of aromatic –C=C- double bonds with shifting was found in PMsCur spectrum, as it was absent in Pluronic F127. This was proved the interaction between curcumin and Pluronic F127 as well as the encapsulation of drug in the core of Pluronic F127 micelles.

Similarly, the XRD study was further carried out to investigate the behavior of curcumin in PMsCur (Fig.2.10). The several characteristic peaks of pure curcumin demonstrated the traits of high crystalline structure. The presence of two characters with high intensity at 2θ angles of 19.8° and 23.8° in the XRD pattern of Pluronic F127 was found due to the PEO groups of the polymer. The absence, broadening, and reduction of majority peaks of curcumin was found in the XRD spectrum of PMsCur. Not only that the two major peaks of PEO groups of Pluronic F127 was also intact with less intensity. The spectrums have confirmed the incorporation of drug into Pluronic F127 micelles.

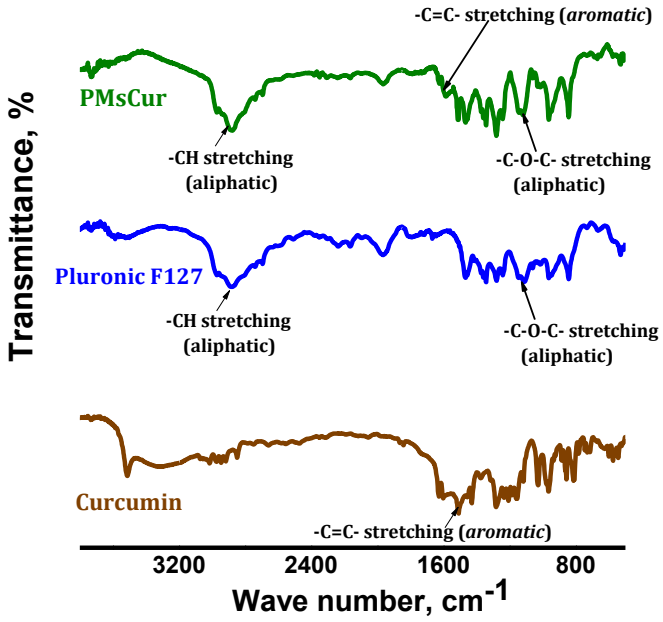

Fig.2.9: FTIR spectra of curcumin, Pluronic F127, and PMsCur.

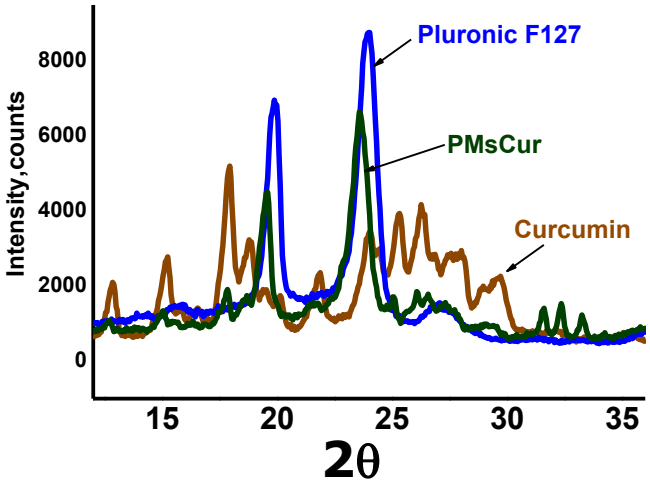

Fig.2.10: XRD patterns of curcumin, Pluronic F127, and PMsCur.

The DSC curves of Pluronic F127, curcumin drug and curcumin incorporated Pluronic micelles (PMsCur) was shown in Fig.2.11. The pure curcumin shows a sharp melting endothermic peak (Tm) at 176°C. The Pluronic F127 showed a peek at 59˚C, referring to the relaxation peak that follows the glass transition. No distinct peak of any melting of a polymer was observed in case of Pluronic F127. The PMsCur curve was somewhat similar to pure Pluronic and not detect any peak at nearby 176˚C, melting of curcumin. It was observed that the microencapsulation process of a drug in PMsCur did not affect the polymer structure. Like FTIR and XRD, the DSC data also proved the incorporation of curcumin drug into micelles of Pluronic F127.

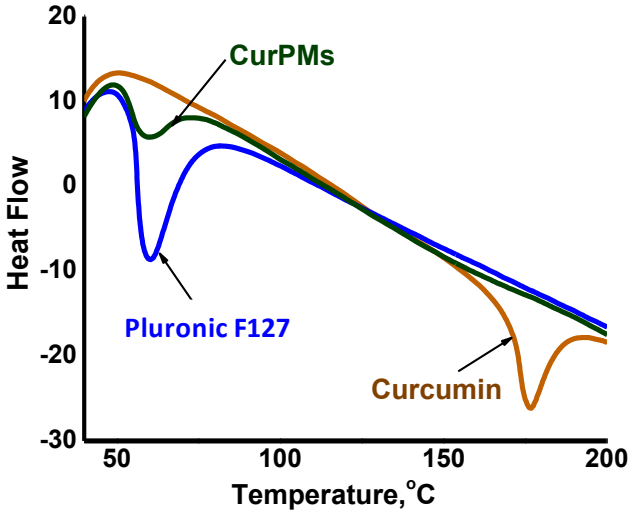

Fig.2.11: DSC of Curcumin, Pluronic F127, and PMsCur.

2.3.5: In-vitro release and stability of PMsCur

Pluronic micelles are known to have a basic feature for slow and sustained release of drug from micelle [54]. Therefore, we have monitored the release of curcumin from PMsCur and found that PMsCur exhibits a slow and sustained release of curcumin at physiological pH. Our study indicates that the encapsulation of curcumin into Pluronic micelles increases its chemical stability in water and slows down its metabolism. These results suggest that PMsCur augments the slow and sustained release of curcumin in cancer cells.

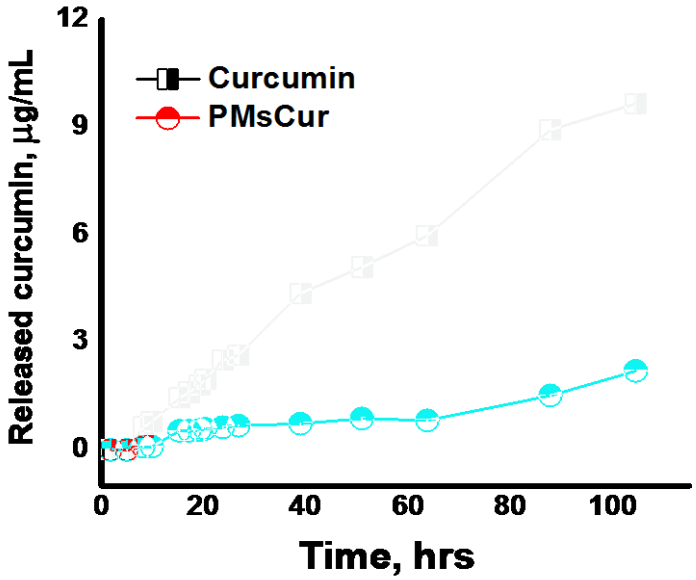

Fig.2.12: In-vitro release of blank curcumin, and PMsCur.

The storage stability of the freeze-dried formulation of PMsCur has been tested for 3 months. The solubility of curcumin at a specific time interval was monitored using the UV-Visible spectroscopy. The data showed that the solubility of curcumin remained unchanged within the studied time period (Fig.2.13). The retention of curcumin was intact in PMsCur, which proves better stability without using any cryoprotectants.

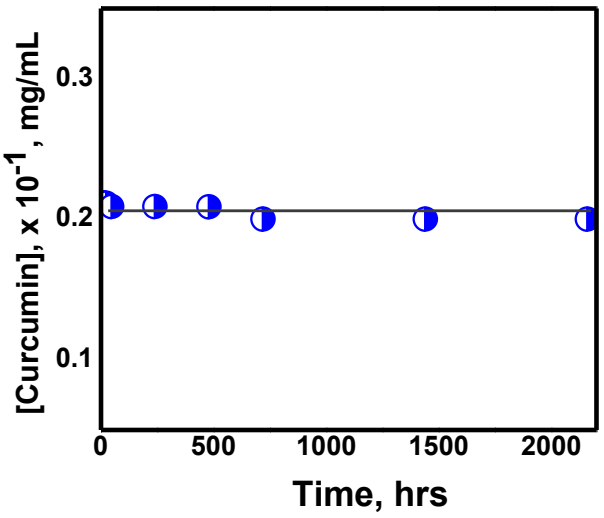

Fig.2.13: Stability Study of PMsCur.

2.4. References

1) Berry, W. R., The evolving role of chemotherapy in androgen-independent (hormone-refractory) prostate cancer. *Urology*, 65(6), **2005**, 2-7.
2) Oh, W. K., Tay, M. H., Huang, J., Is there a role for platinum chemotherapy in the treatment of patients with hormone-refractory prostate cancer? *Cancer*, 109(3), **2007**, 477-486.
3) Petrylak, D.P., Future directions in the treatment of androgen-independent prostate cancer. *Urology*, 65(6), **2005,** 8-12.
4) Urakami, S., Shiina, H., Sumura, M., Honda, S., Wake, K., Hiraoka, T., Inoue, S., Ishikawa, N., Igawa, M., Long-term control or possible cure? Treatment of stage D2 prostate cancer under chemotherapy using cisplatin and estramustine phosphate followed by maximal androgen blockade. *Int. Uro. Nephro*., 40(2), **2008**, 365-368.
5) Agrawal, D.K., Mishra, P.K., Curcumin and its analogues: potential anticancer agents. *Med. Res. Rev*., 30(5), **2010**, 818-860.
6) Anand, P., Kunnumakkara, A.B., Newman, R. A., Aggarwal, B.B., Bioavailability of curcumin: problems and promises. *Mol. Pharma.*, 4(6), **2007**, 807-818.
7) Salem, M., Rohani, S., Gillies, E.R., Curcumin, a promising anti-cancer therapeutic: a review of its chemical properties, bioactivity and approaches to cancer cell delivery. *RSC Adv*., 4(21), **2014**, 10815-10829.
8) Bar-Sela, G., Epelbaum, R., Schaffer, M., Curcumin as an anti-cancer agent: review of the gap between basic and clinical applications. *Curr. Med. Chem*., 17(3), **2010**, 190-197.
9) Jurenka, J.S., Anti-inflammatory properties of curcumin, a major constituent of Curcuma longa: a review of preclinical and clinical research. *Alt. Med. Rev*., 14(2), **2009**, 141-154.
10) Strimpakos, A.S., Sharma, R.A., Curcumin: preventive and therapeutic properties in laboratory studies and clinical trials. *Antioxi. Red. Sign.*, 10(3), **2008**, 511-546.
11) Sharma, R.A., Steward, W.P., Gescher, A.J., Pharmacokinetics and pharmacodynamics of curcumin. In The molecular targets and therapeutic uses of curcumin in health and disease, *Springer*, Boston, MA., **2007**, 453-470.

12) Karewicz, A., Bielska, D., Gzyl-Malcher, B., Kepczynski, M., Lach, R. and Nowakowska, M., Interaction of curcumin with lipid monolayers and liposomal bilayers. *Colloids Surf B: Bio.*, 88(1), **2011**, 231-239.

13) Yallapu, M.M., Jaggi, M., Chauhan, S.C., β-Cyclodextrin-curcumin self-assembly enhances curcumin delivery in prostate cancer cells. *Colloids Surf B. Bio*., 79(1), **2010**, 113-125.

14) Cui, J., Yu, B., Zhao, Y., Zhu, W., Li, H., Lou, H., Zhai, G., Enhancement of oral absorption of curcumin by self-micro emulsifying drug delivery systems. *Int. J. Pharma.*, 371(1-2), **2009**, 148-155.

15) Tønnesen, H.H., Karlsen, J., Studies on curcumin and curcuminoids. *Zeitschr. Lebens.-Unters. Forschung*, 180(5), **1985**, 402-404.

16) Tønnesen, H.H., Másson, M., Loftsson, T., Studies of curcumin and curcuminoids. XXVII. Cyclodextrin complexation: solubility, chemical and photochemical stability. *Int. J. Pharma*, 244(1-2), **2002**, 127-135.

17) Sun, M., Gao, Y., Pei, Y., Guo, C., Li, H., Cao, F., Yu, A., Zhai, G., Development of nanosuspension formulation for oral delivery of quercetin. *J. Biomed. Nanotech*., 6(4), **2010**, 325-332.

18) Yallapu, M.M., Gupta, B.K., Jaggi, M., Chauhan, S.C., Fabrication of curcumin encapsulated PLGA nanoparticles for improved therapeutic effects in metastatic cancer cells. *J. Colloid Int. Sci*., 351(1), **2010**, 19-29.

19) Suwannateep, N., Banlunara, W., Wanichwecharungruang, S.P., Chiablaem, K., Lirdprapamongkol, K., Svasti, J., Mucoadhesive curcumin nanospheres: biological activity, adhesion to stomach mucosa and release of curcumin into the circulation. *J. Cont. Rel.*, 151(2), **2011**, 176-182.

20) Rejinold, N.S., Muthunarayanan, M., Divyarani, V.V., Sreerekha, P.R., Chennazhi, K.P., Nair, S.V., Tamura, H., Jayakumar, R., Curcumin-loaded biocompatible thermoresponsive polymeric nanoparticles for cancer drug delivery. *J. Colloid Int. Sci*, 360(1), **2011**, 39-51.

21) Nishiyama, N., Kataoka, K., Current state, achievements, and future prospects of polymeric micelles as nanocarriers for drug and gene delivery. *Pharma. Ther.*, 112(3), **2006**, 630-648.

22) Chiappetta, D.A., Sosnik, A., Poly (ethylene oxide)–poly (propylene oxide) block copolymer micelles as drug delivery agents: improved hydrosolubility, stability and bioavailability of drugs. *Eur. J. Pharma. Biopharma.*, 66(3), **2007**, 303-317.

23) http://worldaccount.basf.com/wa/NAFTA/Catalog/ChemicalsNAFTA/pi/BASF/Brand/Pluronic

24) Brown, W., Schillen, K., Almgren, M., Hvidt, S., Bahadur, P., Micelle and gel formation in a poly (ethylene oxide)/poly (propylene oxide)/poly (ethylene oxide) triblock copolymer in water solution: dynamic and static light scattering and oscillatory shear measurements. *J. Phys. Chem.*, 95(4), **1991**, 1850-1858.

25) Batrakova, E.V., Kabanov, A.V., Pluronic block copolymers: evolution of drug delivery concept from inert nanocarriers to biological response modifiers. *J. Cont. Rel.*, 130(2), **2008**, 98-106.

26) Oh, K.T., Bronich, T.K., Kabanov, A.V., Micellar formulations for drug delivery based on mixtures of hydrophobic and hydrophilic Pluronic block copolymers. *J. Cont. Rel.*, 94(2-3), **2004**, 411-422.

27) Pitto-Barry, A., Barry, N.P., Pluronic block-copolymers in medicine: from chemical and biological versatility to rationalisation and clinical advances. *Poly. Chem.*, 5(10), **2014**, 3291-3297.

28) Kabanov, A.V., Batrakova, E.V., Alakhov, V.Y., Pluronic block copolymers as novel polymer therapeutics for drug and gene delivery. *J. Cont. Rel.*,82(2-3), **2002**, 189-212.

29) Sahu, A., Kasoju, N., Goswami, P., Bora, U., Encapsulation of curcumin in Pluronic block copolymer micelles for drug delivery applications. *J. Biomat. App.*, 25(6), **2011**, 619-639.

30) Singh, R., Kristensen, S.,Tønnesen, H.H., Influence of cosolvents, ionic strength and the method of sample preparation on the solubilization of curcumin by Pluronics and HP-γ-cyclodextrin studies of curcumin and curcuminoids, XLIV. *Die Pharmazie-An Int. J. Pharma. Sci.*, 67(2), **2012**, 131-142.

31) Mohanty, C., Sahoo, S.K., The in vitro stability and in vivo pharmacokinetics of curcumin prepared as an aqueous nanoparticulate formulation. *Biomaterials*, 31(25), **2010**, 6597-6611.

32) Zhao, L., Du, J., Duan, Y., Zhang, H., Yang, C., Cao, F.,Zhai, G., Curcumin loaded mixed micelles composed of Pluronic P123 and F68: preparation, optimization and in vitro characterization. *Colloids Surf B. Bio*. 97, **2012,** 101-108.

33) Samanta, S., Roccatano, D., Interaction of curcumin with PEO–PPO–PEO block copolymers: a molecular dynamics study. *J.Phy. Chem. B*, 117(11), **2013**, 3250-3257.

34) Ray, G.B., Chakraborty, I., Moulik, S.P., Pyrene absorption can be a convenient method for probing critical micellar concentration (CMC) and indexing micellar polarity. *J. Colloid Int. Sci.*, 294(1), **2006**, 248-254.

35) Aswal, V.K., Goyal, P.S., Small-angle neutron scattering diffractometer at Dhruva reactor. *Curr.Sci.*, 79(7), **2000**, 947-953.

36) Hayter, J.B., Penfold, J., Determination of micelle structure and charge by neutron small-angle scattering. *Colloid Poly. Sci*., 261(12), **1983**, 1022-1030.

37) Kaler, E.W., Small-angle scattering from colloidal dispersions. *J. App. Crys*., 21(6), **1988**, 729-736.

38) Pedersen, J.S., Form factors of block copolymer micelles with spherical, ellipsoidal and cylindrical cores. *J. App. Crys*., 33(3), **2000**, 637-640.

39) Percus, J.K. Yevick, G.J., Analysis of classical statistical mechanics by means of collective coordinates. *Phy. Rev.*,110(1), **1958**. 1.

40) Pedersen, J.S., Analysis of small-angle scattering data from colloids and polymer solutions: modeling and least-squares fitting. *Adv. Colloid int. Sci*., 70, **1997**, 171-210.

41) Pedersen, J.S., Riekel, C., Resolution function and flux at the sample for small-angle X-ray scattering calculated in position–angle–wavelength space. *J. App. Crys*., 24(5), **1991**, 893-909.

42) Bevington, P.R., Robinson, D.K., Blair, J.M., Mallinckrodt, A.J., McKay, S., Data reduction and error analysis for the physical sciences. *Comp. in Phy*., 7(4), **1993**, 415-416.

43) Sharma, P.K., Bhatia, S.R., Effect of anti-inflammatories on Pluronic F127: micellar assembly, gelation and partitioning. *Int. J. Pharma.*, 278(2), **2004**, 361-377.

44) Zhang, Y., Lam, Y.M., Controlled synthesis and association behavior of graft Pluronic in aqueous solutions. *J. Colloid Int. Sci.*, 306(2), **2007**, 398-404.

45) Attwood, D., Tadros, T.F., Tadros, T.F., Colloid stability and application in pharmacy. *Wiley, Weinheim*, 3, **2007**, 61-78.

46) Holmqvist, P., Alexandridis, P., Lindman, B., Modification of the microstructure in poloxamer block copolymer water "oil" systems by varying the "oil" type. *Macromolecules*, 30(22), **1997**, 6788-6797.

47) Ivanova, R., Lindman, B., Alexandridis, P., Evolution in structural polymorphism of Pluronic F127 poly (ethylene oxide)− poly (propylene oxide) block copolymer in ternary systems with water and pharmaceutically acceptable organic solvents: from "glycols" to "oils". *Langmuir*, 16(23), **2000**, 9058-9069.

48) Ivanova, R., Lindman, B., Alexandridis, P., Effect of pharmaceutically acceptable glycols on the stability of the liquid crystalline gels formed by poloxamer 407 in water. *J. Colloid Int. Sci.*, 252(1), **2002**, 226-235.

49) Alexandridis, P., Holzwarth, J.F., Hatton, T.A., Micellization of poly (ethylene oxide)-poly (propylene oxide)-poly (ethylene oxide) triblock copolymers in aqueous solutions: thermodynamics of copolymer association. *Macromolecules*, 27(9), **1994**, 2414-2425.

50) Desai, P.R., Jain, N.J., Sharma, R.K., Bahadur, P., Effect of additives on the micellization of PEO/PPO/PEO block copolymer F127 in aqueous solution. *Colloids Surf. A: Phys. Engg. Asp*., 178(1-3), **2001**, 57-69.

51) Müller, R.H., Colloidal carriers for controlled drug delivery and targeting: modification, characterization and in vivo distribution. *Taylor & Francis.*,**1991**.

52) Alexandridis, P., Yang, L., SANS investigation of polyether block copolymer micelle structure in mixed solvents of water and formamide, ethanol, or glycerol. *Macromolecules*, 33(15), **2000**, 5574-5587.

53) Jain, N.J., Aswal, V.K., Goyal, P.S., Bahadur, P., Micellar structure of an ethylene oxide-propylene oxide block copolymer: a small-angle neutron scattering study. *J. Phy. Chem. B*, 102(43), **1998**, 8452-8458.

54) Yang, X., Li, Z., Wang, N., Li, L., Song, L., He, T., Sun, L., Wang, Z., Wu, Q., Luo, N., Yi, C., Curcumin-encapsulated polymeric micelles suppress the development of colon cancer in vitro and in vivo. *Sci. Rep.*, 5, **2015**, 10322.